A&A 380, L39–L42 (2001)
DOI: 10.1051/0004-6361:20011548

Astronomy & Astrophysics

Signatures of very long period waves in the polar coronal holes

D. Banerjee[1], E. O'Shea[2], J. G. Doyle[3], and M. Goossens[1]

[1] Centre for Plasma Astrophysics, Katholieke Universiteit Leuven, Celestijnenlaan 200B, 3001 Heverlee, Belgium
e-mail: Marcel.Goossens@wis.kuleuven.ac.be
[2] ESA Space Science Dept, ESTEC Solar System Div., Keplerlaan 1, 2201 AZ, Noordwijk, The Netherlands
e-mail: eoshea@so.estec.esa.nl
[3] Armagh Observatory, College Hill, Armagh BT61 9DG, N. Ireland
e-mail: jgd@star.arm.ac.uk

Received 17 September 2001 / Accepted 8 November 2001

Abstract. We examine long spectral time series of a coronal hole observed on the 7th March 2000 with the Coronal Diagnostic Spectrometer (CDS) on-board SoHO. The observations were obtained in the chromospheric He I, and a series of higher temperature oxygen lines. In this letter we report on the presence of long period oscillations in a polar coronal hole region on the disk. Our observations indicate the presence of compressional waves with periods of 20–30 min or longer.

Key words. Sun: polar coronal holes – ultraviolet: SoHO – Sun: oscillations

1. Introduction

Coronal holes in the solar atmosphere have been identified as the source regions of the fast solar wind. Recent observations from SUMER/SoHO have also shown that the coronal velocity structure is linked with the chromospheric magnetic network, with the largest outflow velocities occurring along network boundaries (Hassler et al. 1999). Wilhelm et al. (2000) reported more blue-shifts inside than outside coronal holes. They also showed that the outflow of material, which must occur through open field lines, occurs mostly in the darker regions. Thus it is becoming increasingly important to study the dynamics of the polar coronal hole regions. Banerjee et al. (2000) investigated the temporal behaviour of polar plumes as observed in the transition region line O V 629 Å line, noting the presence of long period (20–30 min) compressional waves. In a follow-up paper, Banerjee et al. (2001) extended this study to the inter-plume regions and reported on even longer periodicities (up to 70 min) over a wider temperature range. It is also becoming important to know whether one can find different types of waves in these different regions, namely the plume, the inter-plume and the coronal hole. Also, one needs to address the question of whether the long period waves observed outside the limb (in the plume and inter-plume) originate from the disk part of the coronal hole? In this letter we report on the temporal behaviour of a polar coronal hole as observed by the CDS/SoHO instrument.

Send offprint requests to: D. Banerjee,
e-mail: dipu@wis.kuleuven.ac.be

2. Observations and data reduction

For these observations we have used the normal incidence spectrometer (NIS) (Harrison et al. 1995), which is one of the components of the Coronal Diagnostic Spectrometer (CDS) on-board the Solar Heliospheric Observatory (SoHO). In order to get good time resolution the rotational compensation was switched off (sit-and-stare mode) and so it is important to calculate the lowest possible frequency we can detect from this long time sequence after taking the solar rotation into account (see Doyle et al. 1998 for details). For our dataset, s18778r00 (coordinates $x = 127$, $y = 781$), this rotation amounts to 3 arcsec per hour. Thus for a 2 arcsec wide slit width, the lowest frequency resolution is 0.42 mHz. The temporal series dataset was obtained on 7th March 2000 for the four lines of He I 584 Å, O III 599 Å, O IV 554 Å and O V 629 Å, with exposure times of 60 sec and using the 2 × 240 arcsec slit. The formation temperature of these lines range from 20 000K to 250 000K. We fit the O IV 554 Å line with three Gaussians to take account of the two weaker components of the multiplet at ∼553 and 555 Å. In all other cases, fitting was done using a single Gaussian as the lines were found to be generally symmetric. Details on the CDS reduction procedure, plus the wavelet analysis, may be found in O'Shea et al. (2001). Before applying the wavelet analysis we first removed the trend of

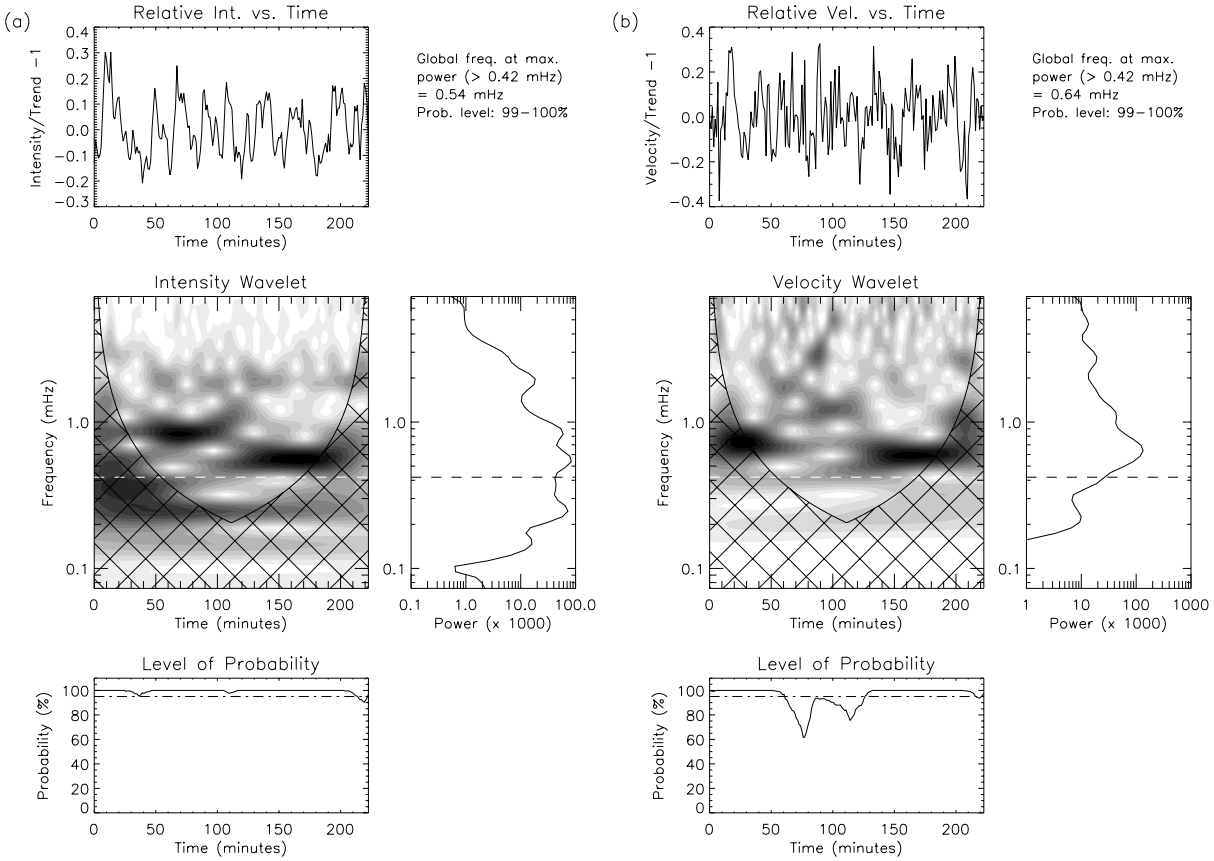

Fig. 1. Wavelet results corresponding to the He I 584 Å line in the s18778r00 dataset at pixel 22. Panels **a)** and **b)** represent intensity and velocity results respectively. The middle row left panels show the time frequency phase plot corresponding to the variations shown in the top panels. The middle row right hand panels show the average of the wavelet power spectrum over time, i.e. the global wavelet spectrum. The continuous dashed horizontal lines in the wavelet spectra indicate the lower cut off frequency (∼0.42 mHz). The lowest panels show the variation of the probability with time from the randomisation test, with the dot-dash line indicating the 95% significance level.

the data (i.e. the very lowest frequency oscillations) using a 30 point running average. By dividing the results of this running average (or trend) into the original data and subtracting a value of one we obtained the resulting detrended data used in the analysis. The statistical significance of the observed oscillations was estimated using a Monte Carlo or randomisation method. The advantage of using a randomisation test is that it is distribution free or nonparametric, i.e. it is not limited or constrained by any specific noise models, such as Poisson, Gaussian etc. We follow the method of Fisher randomisation as outlined in Nemec & Nemec (1985), performing 250 random permutations to calculate the probability levels. The levels displayed here are the values of $(1-p)\times 100$, where p is the proportion of the permutations that show a null test result (see O'Shea et al. 2001). We choose a value of 95% as the lowest acceptable probability level. Occasionally the *estimated* p value can have a value of zero, i.e. there being an almost zero chance that the observed time series oscillations could have occurred by chance. In this case, and following Nemec & Nemec (1985), the 95% confidence interval can be obtained using the binomial distribution, and is given by $0.0 < p < 0.01$, that is, the probability $((1-p)\times 100)$ in this case is between 99–100%. To improve the signal-to-noise ratio of this data we binned by three pixels along the slit, in effect creating new pixels of $\sim 5\times 2$ arcsec^2. The velocity values presented in this letter are relative velocities, that is, they are calculated relative to an averaged profile, obtained by summing over all pixels along the slit and all time frames.

3. Results

The He I 584 Å results are presented in Fig 1. In the wavelet spectrum, the dark contour regions show the locations of the highest powers. Only locations that have a probability greater than 95% are regarded as being real, i.e. not due to noise. Cross-hatched regions, on either side of the wavelet spectrum, indicate the "cone of influence" (COI), where edge effects become important (see Torrence & Compo 1998). The dashed horizontal lines in the wavelet spectra indicate the lower frequency cut-off, in this instance 0.42 mHz, corresponding to oscillations with periods of ∼40 min. The results from the phase plots show that the He I 584 Å intensity and velocity both show significant power in the 0.5–0.8 mHz range, for almost the entire

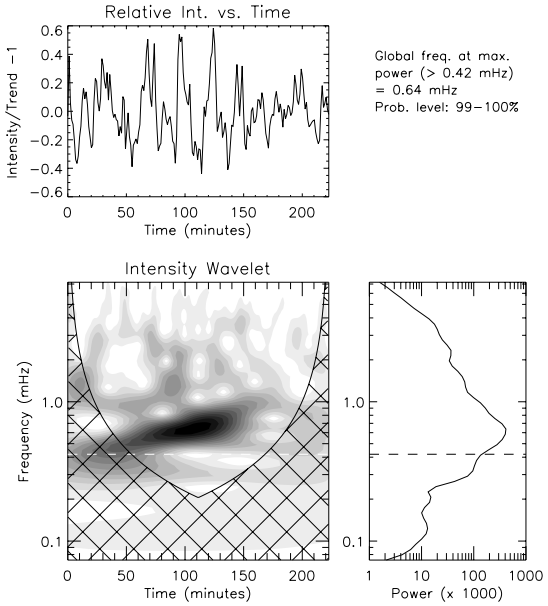

Fig. 2. Intensity wavelet results for the O III 599 Å line corresponding to pixel location 28.

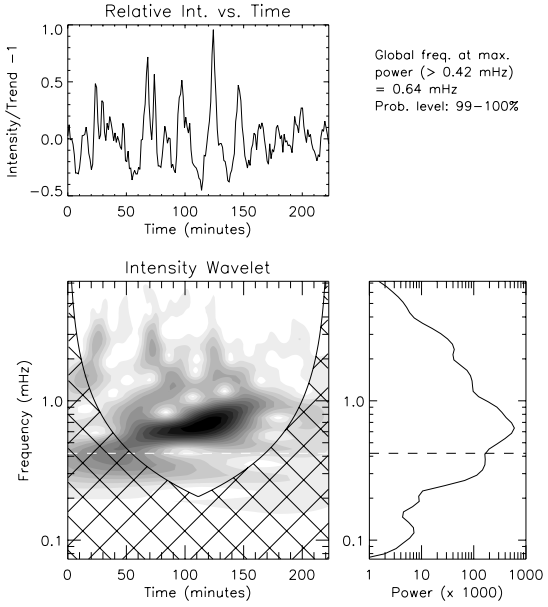

Fig. 3. Intensity wavelet results for the O IV 554 Å line corresponding to pixel location 28.

observing period. The global wavelet spectra (on the right of Figs. 1a and b), which are the average of the wavelet power spectrum over the entire observing period, show the strongest intensity power at 0.54 mHz (∼31 min) and the strongest velocity power at 0.64 mHz (∼26 min). This is printed out in Fig. 1 above the global wavelet plots, together with the probability estimate for the global wavelet power spectrum.

Turning to the higher temperature oxygen lines, the intensity wavelet results of O III 599 Å, O IV 554 Å and O V 629 Å are presented in Figs. 2, 3 and 4 respectively, for a single pixel location, px 28. All three oxygen lines show

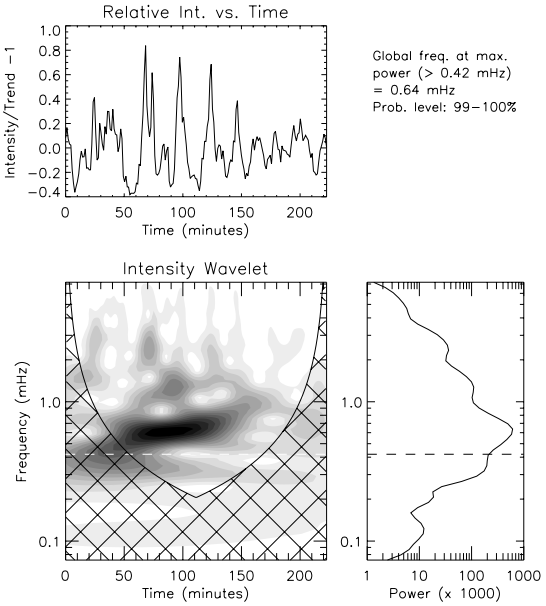

Fig. 4. Intensity wavelet results for the O V 629 Å line corresponding to pixel location 28.

intensity power around 0.7 mHz, with a peak at 0.64 mHz, in the global wavelet spectrum plots, at a very high probability level (see value in figures). The velocity oscillation shows a similar trend but with a much smaller probability level. For the O V velocity data, the strongest global peak is at 0.7 mHz, with a 99.6% probability level. For the other two oxygen lines the velocity oscillations are much weaker and are not considered to be significant. Note that the nature and period of the intensity oscillations, corresponding to the three oxygen lines, formed over the temperature range 100 000 to 250 000 K, behave more or less in a similar way.

To emphasize the fact that these low frequency oscillations are not only coming from one or two particular pixel locations but rather from all over the coronal hole across our slit, we show, in Fig. 5, the spatial behaviour of the oscillation frequencies measured from the O V 629 Å line for a section of the slit. This figure shows the measured frequencies as a function of position along the slit (X-F slice). The frequencies in the left panels, crosses and plus symbols, correspond to the primary and secondary maxima (from the global wavelet spectrum) respectively. The total number of counts in a pixel (summed counts) during the observation is shown in the right column, and is useful in identifying the network brightening (the peaks correspond to the network pixels). The intensity and velocity results both show that the primary maxima in the global wavelet spectra lies in the range 0.5–1.0 mHz. The secondary maxima of intensity often appears in the 1.2–1.4 mHz range. The appearance of a few more crosses in the intensity X-F slice as compared to the velocity also indicates that the intensity oscillations are slightly stronger and more reliable (>95% probability level). Note that these low frequency oscillations come from both bright and dark pixels, implying that they are present both in the network and

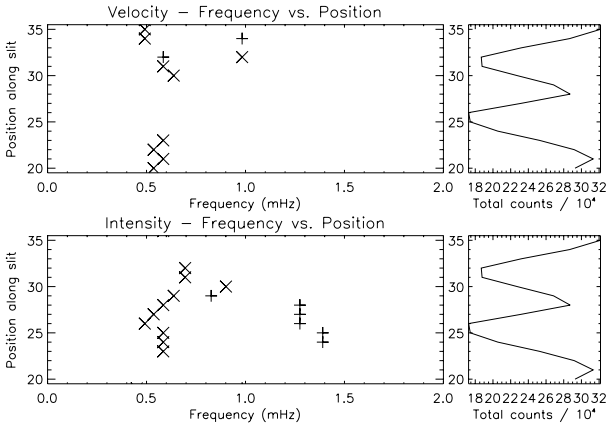

Fig. 5. Frequencies measured as a function of spatial position along the slit (X-F slice) for the O v 629Å line (left panels). The right panels show the total number of counts in a pixel (summed counts) over the observation time.

internetwork, if that structure is present in the coronal hole.

4. Conclusion

High-cadence EIT/SoHO observations indicate that quasi periodic fluctuations with periods of 10–15 min are present in polar plumes (DeForest & Gurman 1998). These authors conclude that the fluctuations are caused either by sound waves or slow magneto-acoustic waves propagating along the plumes at ∼75–150 $\mathrm{km\,s^{-1}}$. Ofman et al. (2000) detected quasi periodic variations in the polarization brightness (pB) at 1.9 $R_\odot$, in both plume and inter-plume regions. Their Fourier power spectrum shows significant peaks around 1.6–2.5 mHz and additional smaller peaks at longer and shorter time-scales. Recently, Banerjee et al. (2000, 2001) reported on the existence of long period slow magneto-acoustic waves in the plumes and inter-plumes respectively, as observed by CDS/SoHO. Compressional modes reveal themselves in the form of intensity oscillations, through variations in the emission measure, and also as velocity oscillations through fluctuations in the plasma density. This fact allowed them to interpret the measured oscillations as being due to slow magneto-acoustic waves. It is likely that the waves detected at 1.9 $R_\odot$ by Ofman et al. (2000) using UVCS/SoHO and the waves detected by DeForest & Gurman (1998) around 1.2 $R_\odot$ using EIT/SoHO are the same as those reported by Banerjee et al. (2000, 2001) in the polar plumes and inter-plumes very close to the solar limb (off-limb). Thus it is important to find a source region for these long period waves.

It was conjectured that these waves can originate from the network boundaries in the polar coronal hole. In this short contribution we show that these long period waves do indeed originate from the disk part of the coronal hole but the important point to note is that they are also present at several locations in the coronal hole, namely in the network and internetwork regions. We find the presence of long period oscillations in bright pixels (corresponding to the network locations) and also in the darker pixels corresponding to the inter-network. The nature of the waves are very similar to the ones reported by Banerjee et al. (2000, 2001) and thus we also interpret these waves as slow magneto-acoustic. We should also point out here that we do not have information about the phase speed, k and the phase relations, which confirms if the waves are slow or fast. But since we do not observe any steepening of the wave amplitudes or shocks we suggest that these waves are slow waves. Furthermore, it is interesting to note that these long period slow waves are detected in plasma ranging in temperature from 20 000 K to 250 000 K, which implies that theses waves are present much lower in the atmosphere and are able to propagate upwards. However, we have not been able to pin-point the location where these waves originate and whether they are present in the corona. We hope to address these questions in a wider diagnostic study in a future observing campaign.

Acknowledgements. DB wishes to thank the ONDERZOEKSRAAD of K.U. Leuven for a fellowship (F/99/42). EOS is a member of the European Solar Magnetometry Network (`www.astro.su.se/~dorch/esmn/`). We would like to thank the CDS and EIT teams at Goddard Space Flight Center for their help in obtaining the present data. CDS and EIT are part of SoHO, the Solar and Heliospheric Observatory, which is a mission of international cooperation between ESA and NASA. Research at Armagh Observatory is grant-aided by the N. Ireland Dept. of Culture, Arts and Leisure. This work was supported by PPARC grant PPA/G/S/1999/00055. The original wavelet software was provided by C. Torrence and G. Compo, and is available at URL: `http://paos.colorado.edu/research/wavelets/`

References

Banerjee, D., O'Shea, E., Doyle, J. G., & Goossens, M. 2001, A&A, 377, 691
Banerjee, D., O'Shea, E. , & Doyle, J. G. 2000, Sol. Phys., 196, 63
DeForest, C. E., & Gurman, J. B. 1998, ApJ, 501, L217
Doyle, J. G., van den Oord, G. H. J., O'Shea, E., & Banerjee, D. 1998, Sol. Phys., 181, 51
Harrison, R. A., Sawyer, E. C., Carter, M. K., et al. 1995, Sol. Phys., 162, 233
Hassler, D. M., Dammasch, I. E., Lemaire, P., et al. 1999, Science, 283, 810
Nemec, A. F., & Nemec, J. M. 1985, AJ, 90, 2317
Ofman, L., Romali, M., Poletto, G., Noci, G., & Kohl, J. L. 2000, ApJ, 529, 592
O'Shea, E., Banerjee, D., Doyle, J. G., Fleck, B., & Murtagh, F. 2001, A&A, 368, 1095
Torrence, C., & Compo, G. P. 1998, Bull. Amer. Meteor. Soc., 79, 61
Wilhelm, K., Dammasch, I. E., Marsch, E., & Hassler, D. M. 2000, A&A, 353, 749